Zhai, Z. and Chen, Q. 2003. "Solution characters of iterative coupling between energy simulation and CFD programs," *Energy and Buildings*, 35(5), 493-505.

Solution characters of iterative coupling between energy simulation and CFD programs

Zhiqiang Zhai[a], Qingyan (Yan) Chen[b,*]

[a)] Building Technology Program, Massachusetts Institute of Technology, Room 5-418, 77 Massachusetts Avenue, Cambridge, MA 02139-4307, USA

[b)] School of Mechanical Engineering, Purdue University, 1288 Mechanical Engineering Building, West Lafayette, IN 47907-1288, USA

Abstract

Energy simulation (ES) and computational fluid dynamics (CFD) provide important and complementary information for building energy and indoor environment designs. A coupled ES and CFD simulation can eliminate many assumptions employed in the separate ES and CFD computations and thus provide more accurate results. Through theoretical analysis and numerical experiment, this study verified that the solution of a coupled ES and CFD simulation does exist and is unique. The investigation also concluded that a converged and stable simulation can be achieved with three different data coupling methods. The study has further developed an improved iteration and control algorithm for the coupled simulation.

Keyword: Coupling; Energy simulation; CFD

Nomenclature

A	area of surface (m^2)
A	coefficient matrix
B	coefficient matrix
C	contaminant concentration (mg/kg or ppm)
C_p	air specific heat (J/kgK)
f	math function
g	math function
h	heat transfer coefficient (W/m^2K)
IterCFD	CFD iteration number
K	conductivity of wall (W/mK)
L	thickness of wall (m)
N	number of enclosure surfaces
q	heat flux (W/m^2)
Q	total heat flux (W)
Q	interior surface heat convection tensor
R	residual
S	source term
t	time (s)
T	air temperature, surface temperature (K)

* Corresponding author. Tel.: + 1-765- 496-7562, FAX: 1-765- 494-0539
E-mail address: yanchen@purdue.edu (Q. Chen).

T	surface temperature tensor
U	air velocity component (m/s)
V	room volume (m^3)
V	velocity vector

Greek Symbols

ρ	air density (kg/m^3)
Δ	difference
Φ	general variable
Γ	diffusion coefficient (kg/ms)

Subscripts

a	indoor air close to surface
CFD	provided by CFD program
cond	conduction
c, conv	convection
control-cal	calculated control value
control-set	required control value
ES	provided by energy simulation program
extract	heat extraction of space
i, k	index of enclosure surfaces
j	direction of velocity component
o	exterior surface
others	lights, people, appliances, infiltration, etc.
outlet	exhaust air
r, rad	radiation
room	room-averaged
s	interior surface
s-rad	solar radiation and radiation from internal heat sources
supply	supply air

Superscripts

n	nth iteration step
n+1	(n+1)th iteration step

1. Introduction

In the United States, building services consume more than one third of the primary energy consumption and two thirds of the electricity. Designing an energy-efficient building requires an accurate estimate of the building's energy use during the design stage. Meanwhile, an energy-efficient building should also be thermally comfortable and have acceptable indoor air quality.

Estimation of building energy usage normally uses manual methods, such as the degree-day and bin methods [1], as well as computer simulation methods. Generally, manual methods cannot produce accurate results and cannot handle a complicated

heating, ventilating and air conditioning (HVAC) system. On the other hand, computer simulation of energy usage in buildings by advanced energy simulation (ES) programs, such as TRNSYS [2], BLAST [3], DOE-2 [4], ESP-r [5], and EnergyPlus [6], can provide detailed energy information for a whole building and the HVAC systems used. Space-averaged indoor environmental conditions, cooling/heating loads, coil loads, and energy consumption can be obtained on an hourly or sub-hourly basis for a period of time ranging from a design day to a reference year. The computational results are more accurate and informative than those obtained with the manual methods, and therefore, energy simulation programs are widely used in design practice.

However, ES often assumes that room air is well-mixed and uses empirical formulas to estimate the convective heat transfer between the room air and the enclosure interior surfaces. In addition, the thermal comfort predicted by ES with the well-mixing assumption is not satisfactory. This is especially evident for stratified indoor environments (e.g. rooms with displacement ventilation) and for spaces with flows different from that used to obtain the empirical equations. Furthermore, ES does not normally calculate indoor air quality. On the contrary, an airflow model could provide more detailed information that can be used to determine thermal comfort and indoor air quality levels in a room. But the airflow models need some thermal and flow boundary conditions, such as wall surface temperature and heat extraction that can be provided by ES. Hence, it seems very attractive to combine an air movement model with an energy simulation model.

Nodal and zonal models were the first generation of airflow models used to estimate the air temperature distribution. In a nodal model, a specific airflow configuration is assumed, and mass and energy balances are written for each node. Lebrun [7] was apparently the first to propose a nodal model for providing a rough estimate of thermal stratification in the context of building energy use. The work focused on modeling how heat is convected around a room by a baseboard heater under a cold window. Some recent nodal models, such as those from [8-10], can predict the vertical temperature gradient in rooms with displacement ventilation. However, these types of models need prior knowledge of the airflow patterns in order to specify mass flow in the thermal network, and are therefore difficult for most designers to use.

Zonal modeling attempts to account for how flow rates might change based on temperature differences, length scales, and initial momentum. Dalicieux and Bouia [11] were apparently the first to publish what is termed a pressure-zonal model that uses pressure as a state variable and solves energy and mass balance equations in the context of building room air modeling. Inard et al. [12] demonstrated a functional three-dimensional pressure zonal model with special cells for walls, jets, and plumes. Other pressure-zonal models are also available, such as [13,14]. Zonal models provide increased generality compared to nodal models. A difficulty in applying pressure-zonal models to general building simulation is the requirement of using special laws to describe flows in certain regions. Furthermore, Griffith [15] found that many zonal models are not numerically stable. Hence, nodal and zonal models are difficult to use without further development.

Computational fluid dynamics (CFD) is the most sophisticated type of airflow models. CFD predicts the detailed spatial distributions of velocity, temperature and contaminants by solving the flow governing equations. In the last two decades, CFD has

been successfully applied to the indoor airflow analysis, as reviewed by [16-18]. The results are the most accurate and detailed among the airflow models.
Generally, two approaches are available to couple CFD with ES. The first one is to extend CFD to solve heat transfer in solid materials (called conjugate heat transfer method) with an appropriate radiation model, HVAC system models and plant models. The studies [19,20] indicated that this approach is very computationally expensive and would not become a design tool in the near future. An alternative approach is to couple a CFD program with an ES program, where ES handles the heat transfer in enclosures with a large time step (a few minutes to an hour), while CFD simulates the indoor airflow at a specific time step. Such a coupling procedure largely reduces computing time because it does not solve the flow field during the transition from one time step to another [20]. Many applications of this coupling approach [21- 26] have shown improved accuracy in both energy simulations and indoor airflow computations. This is because the integration of ES and CFD eliminates many assumptions employed in the separate applications. For example, CFD can provide ES accurate convective surface heat transfer coefficients and indoor air temperature gradients, which are crucial to the accuracy of building energy calculation. On the other hand, ES can provide CFD interior temperatures of building enclosures and heating/cooling energy requirements as boundary conditions, which is important for the accuracy of CFD results. Thus, a coupled CFD and ES program is a powerful tool for designers to design energy-efficient buildings with acceptable thermal comfort and indoor air quality.

However, Clovis [27] indicated that CFD seems to be the most complex package to be integrated with the whole building simulation package and a careful approach must be exercised when coupling CFD tools with other systemic simulation tools. He pointed out that computing time used by CFD and stability and convergence of numerical methods are two major issues associated with the integration of CFD and ES. Zhai et al. [20] proposed several staged coupling strategies to bridge the disparity of computing time between CFD and ES. These strategies provide reasonably accurate results with an acceptable CFD computing cost. A coupled simulation often requires iteration between ES and CFD to reach a mutually consistent solution. Because different mathematical and numerical methods are employed in ES and CFD programs, solution existence and uniqueness, and convergence and stability of the iterative procedure are always major concerns. This paper tries to address these concerns by theoretical analysis and numerical experiment.

2. Theoretical Analysis

2.1. Fundamentals of ES and CFD program coupling

Most ES programs solve the energy balance equations for building enclosures (walls, windows, floor, and roof)

$$q_{i,cond} + q_{i,s-rad} = \sum_{k=1}^{N} q_{ik,rad} + q_{i,conv} \quad (1)$$

and for indoor air

$$\sum_{i=1}^{N} q_{i,conv} A_i + Q_{others} - Q_{extract} = \frac{\rho V_{room} C_p \Delta T_{room}}{\Delta t} \quad (2)$$

Solution of Eq. (1) provides interior surface temperatures and surface convective heat transfers. With the interior convective heat transfers, Eq. (2) can determine the mean indoor air temperature and heat extraction rate of the space.

CFD, on the other hand, solves the partial differential flow governing equations for mass, momentum, and energy conservation in an indoor space, which can be written in a general form

$$\rho \frac{\partial \Phi}{\partial t} + \rho(\mathbf{V} \bullet \nabla)\Phi - \Gamma_\phi \nabla^2 \Phi = S_\phi \quad (3)$$

where, Φ can be U_j for the air velocity component in the j direction (j = 1, 2, 3), 1 for mass continuity, T for temperature, C for different gas contaminants, κ and ε for turbulence parameters.

The substantial coupling of ES and CFD is between Eqs. (1) and (3), since Eq. (2) is the integral form of Eq. (3) for indoor air energy balance. The convective heat transfer on the interior surfaces links ES and CFD. ES provides space heat extraction rate and enclosure thermal information, such as surface temperatures and/or heat flux, to CFD as inlet and solid surface boundary conditions, while CFD provides accurate interior surface convective heat transfer coefficients to ES.

2.2. Solution Existence and Uniqueness of ES-CFD Program Coupling

The ES-CFD program coupling approach, in principle, is equivalent to a "separated" conjugate heat transfer method. The conjugate heat transfer method solves the assembled total matrix equations for all the energy balance equations of enclosures and indoor air, while the program coupling method solves two separate matrix equations (one for enclosures in ES and another for indoor air in CFD). It is well known that the conjugate heat transfer method generally has a converged and stable solution. The question here is whether the iterative solution of separate matrix equations can provide the same results as that of the assembled total matrix equations from the conjugate heat transfer approach. Clarke et al. [22,28] and Klems [29] discussed this question with different matrix and mathematics theories and obtained a positive answer.

Clarke et al. [22,28] investigated the conflation between the network flow and CFD models and indicated that the conflation of these models can be achieved by maintaining separate solution algorithms for each method based on sparse matrix theory [30]. The connection between the two modeling approaches is then made within regions that each approach considers as its boundary condition. The overall system balance is then achieved through an iterative procedure. The conclusions are also suitable to the ES-CFD coupling since many ES programs also use the network model.

Klems [29] mathematically studied the ES and CFD equations, both of which can be written as $q_c = f(T_s)$. q_c and T_s are the interior surface convective heat flux and surface temperature, which link ES and CFD. Klems analyzed the slopes of $q_c = f(T_s)$ for both ES and CFD, and then determined the possibility of the intersection of these two equations. With elaborate assumptions and mathematical deductions to handle the highly non-linear equation systems, Klems verified that the q_c-T_s curve for CFD probably has a positive slope and may be either concave upward or downward, while the curve for ES has a

negative slope if all of the phenomenological convective coefficients are positive. Otherwise, the curve for ES may have positive slope depending on the dynamics of the particular situation. The shapes of the q_c-T_s curves imply that the intersection of CFD and ES curves is possible, implying the existence of a coupled solution between ES and CFD programs.

This paper addresses the existence and uniqueness of the coupled solution in another manner. Considering the heat transfer on one interior surface in terms of conduction, convection, and radiation, and ignoring the radiative heat flux from internal heat sources and solar radiation, we have in ES

$$\sum h_{k,r}(T - T_k) + h_c(T - T_a) = \frac{K}{L}(T_o - T) \tag{4}$$

$$T = \frac{\sum h_{k,r}T_k + h_c T_a + \frac{K}{L}T_o}{\sum h_{k,r} + h_c + \frac{K}{L}} = \frac{h_c}{\sum h_{k,r} + h_c + \frac{K}{L}}T_a + \frac{\sum h_{k,r}T_k + \frac{K}{L}T_o}{\sum h_{k,r} + h_c + \frac{K}{L}} \tag{5}$$

where, T is the interior surface temperature of the current surface concerned.
For simplicity, we assume: (1) all the coefficients are constant; (2) $h_{k,r}$ and K are greater than zero; and (3) T_k and T_o are independent variables. Then we have

$$\frac{\partial T}{\partial T_a} = \frac{h_c}{\sum h_{k,r} + h_c + \frac{K}{L}} = \begin{Bmatrix} (0,1) & h_c > 0 \\ 0 & h_c = 0 \\ \text{else} & h_c < 0 \end{Bmatrix} \tag{6}$$

or

$$\frac{\partial T_a}{\partial T} = \frac{\sum h_{k,r} + h_c + \frac{K}{L}}{h_c} = \begin{Bmatrix} >1 & h_c > 0 \\ \infty & h_c = 0 \\ <1 & h_c < 0 \end{Bmatrix} \tag{7}$$

Therefore

$$\frac{\partial q_c}{\partial T} = \frac{\partial[h_c(T - T_a)]}{\partial T} = \frac{\partial h_c}{\partial T}(T - T_a) + h_c\frac{\partial(T - T_a)}{\partial T} = h_c(1 - \frac{\partial T_a}{\partial T}) = \begin{Bmatrix} <0 & h_c > 0 \\ 0 & h_c = 0 \\ <0 & h_c < 0 \end{Bmatrix} \tag{8}$$

The situation with $h_c<0$ in this analysis is possible although rare, because $h_c=q_c/(T-T_a)$ and the value of T_a may change with location. A typical example is a space with displacement ventilation, where the near-floor air temperature may be lower than the floor temperature while the upper air temperature may be higher.

Eq. (8) can be understood in physics. Table 1. shows the phenomenal changes of conductive, convective and radiative heat with the interior surface temperature T, if all other conditions are fixed. For example, in the summer, assuming the exterior surface temperature T_o is larger than the interior surface temperature T and other interior surface temperatures T_k are smaller than T, when T increases, the temperature gradient over the wall is decreased. Therefore, the conductive heat through the wall is reduced. On the other hand, the radiative heat is increased due to the larger gradient between this surface temperature and others. As a result, the convective heat from the surface $q_{conv} = q_{cond}$ -

q_{rad} is decreased, which fits the expression of Eq. (8). The same results can be obtained by assuming $T_o<T$ or $T_k>T$.

CFD, on the other hand, focuses on the energy balance of indoor air, with the interior surfaces as the boundaries of the space. We could physically find that for cooling situation, the increase of the interior surface temperature T will increase the convective heat gain q_c (positive) and the air temperature T_a close to the wall. For the heating situation, the decrease of T will increase the convective heat loss q_c (negative) and decrease the air temperature T_a close to the wall.

This means, $\frac{\partial q_c}{\partial T} > 0$ and $\frac{\partial T_a}{\partial T} > 0$. Therefore, with a constant h_c,

$$\frac{\partial q_c}{\partial T} = \frac{\partial [h_c (T - T_a)]}{\partial T} = \frac{\partial h_c}{\partial T}(T - T_a) + h_c \frac{\partial (T - T_a)}{\partial T} = h_c (1 - \frac{\partial T_a}{\partial T}) > 0 \qquad (9)$$

It can be further expressed as

$$1 > \frac{\partial T_a}{\partial T} > 0 \quad \text{when} \quad h_c > 0 \qquad (10a)$$

$$\frac{\partial T_a}{\partial T} > 1 \quad \text{when} \quad h_c < 0 \qquad (10b)$$

Klems [29] defines the condition $\frac{\partial T_a}{\partial T} > 1$ as a super-linear response of the CFD calculation. That is, the change in air temperature caused by the change in surface temperature is larger than the original surface temperature change. Such a response cannot be excluded, although it is uncommon. The q_c-T curve slopes from this analysis (Eqs. (8) and (9)) are partly coincident with those from the verification by Klems. With these slopes of the T_a-T and q_c-T curves, we have the positive intersection for ES and CFD coupling, as shown in Figs. 1 and 2, although the curves are not necessarily straight. The next question is whether there are multiple intersections (solutions) for the ES and CFD coupling. If there were multiple intersections, Fig. 3 shows two possible scenarios with positive h values (similar analysis can be offered for the scenarios with negative h values). Since the T_a-T slope for CFD at $h_c>0$ is between 0 and 1 while that for ES is larger than 1, the scenario shown in Fig. 3(a) is impossible because the slope around point 2 does not satisfy the slope requirement. The scenario shown in Fig. 3(b) is also impossible because one specific surface temperature T in CFD can have only one corresponding T_a for a given situation (including given numerical models and techniques). The same applies to ES. Therefore, there is one and only one solution for ES and CFD coupling.

Although the above analysis assumed constant coefficients and fixed other conditions, it is rather valuable because (1) the analysis provides essential understanding of ES-CFD coupling and the possible solutions; (2) the coefficients in a specific case usually do not change dramatically with time and environmental conditions; (3) the assumption of constant coefficients is used in a number of simulation tools.

2.3. Convergence and Stability of Iterative ES and CFD Coupling

2.3.1. Data exchange methods between ES and CFD

The primary connection in ES and CFD coupling is through convective heat transfer on building envelope. The implementation method of coupling can be multiple. Generally, CFD has three kinds of thermal boundary conditions – given surface temperature T_s (Dirichlet condition), given surface heat flux Q_{conv} (Newmann condition), and given Q_{conv}-T_s relationship (Robbins condition). The third boundary condition describes a relationship between the conduction in solid materials and the convection with neighboring air, which is not suitable for the CFD calculation without considering conduction in the envelope. On the other hand, because the convective heat transfer from interior enclosures is

$$Q_{conv} = h_c A(T_s - T_a) = h_c A[T_s - T_{room} + (T_{room} - T_a)]$$
$$= h_c A(T_s - T_{room} + \Delta T_{room,a}) \quad (11)$$

where $\Delta T_{room,a} = T_{room} - T_a$, ES has two approaches to acquire the thermal information (convection from envelopes) from CFD, by Q_{conv} directly or by h_c and indoor air temperature gradient $\Delta T_{room,a}$.

Therefore, the potential combinations of inter-coupled boundary condition exchanges between ES and CFD are:

- data exchange method-1: ES to CFD by T_s; CFD to ES by h and $\Delta T_{room,a}$;
- data exchange method-2: ES to CFD by T_s; CFD to ES by Q_{conv};
- data exchange method-3: ES to CFD by Q_{conv}; CFD to ES by h and $\Delta T_{room,a}$;
- data exchange method-4: ES to CFD by Q_{conv}; CFD to ES by Q_{conv}.

However, not all the coupling methods are feasible. For example, the Q_{conv} obtained in ES will never be updated in the CFD simulation in method-4 due to the fixed heat flux boundary conditions in CFD. CFD could not provide a new Q_{conv} to ES with this data exchange method. In order to discuss the feasibility of the other three data exchange methods, the following discussion still assumes a constant convective heat transfer coefficient h for simplicity.

In the coupled simulation, CFD replaces the ES zone air energy balance equation to connect with the ES envelope energy balance equation. Iteratively solving these two sets of equations provides the envelope thermal conditions (heat flux and temperature) and indoor air temperature distribution.

The envelope energy balance equation of ES can be expressed in tensor form:

$$\mathbf{AT} = \mathbf{B} + \mathbf{Q} \quad (12)$$

where **T** and **Q** are unknown variables. **Q** can be obtained in CFD with the non-linear energy equations for indoor air

$$\mathbf{Q} = f(\mathbf{T}) \quad (13)$$

Iteratively solving Eqs. (12) and (13) provides the surface temperature T and heat flux Q. This is the basic route of data exchange method-2.

Since $\mathbf{Q} = h(\mathbf{T} - \mathbf{T_a})$, where $\mathbf{T_a}$ is the air temperature close to the surface, substitute it to (12)

$$\mathbf{AT} = \mathbf{B} + h\mathbf{T} - h\mathbf{T_a} \quad (14)$$

Rearrange it to be

$$(\mathbf{A} - h)\mathbf{T} = \mathbf{B} - h\mathbf{T_a} \quad (15)$$

In CFD

$$\mathbf{Q} = f(\mathbf{T}) = h(\mathbf{T} - \mathbf{T_a}) \quad (16)$$

$$\mathbf{T_a}=\mathbf{T}-f(\mathbf{T})/h=g(\mathbf{T}) \quad (17)$$

Eqs. (15) and (17) are the equation group about unknown variables **T** and $\mathbf{T_a}$. They are derived from Eqs. (12) and (13) and therefore exactly the same as (12) and (13) but in different forms. The solutions of (15) and (17) are surface temperature and the air temperature close to the surface. This is data exchange method-1. Method-1, therefore, is mathematically equivalent to method-2.

In data exchange method-3, **Q,** rather than **T**, is transferred from ES to CFD as boundary conditions, therefore in CFD

$$\mathbf{T_a}=f(\mathbf{Q})=g(\mathbf{T}-\mathbf{T_a}) \quad (18)$$

And Eq. (14) can be rewritten as

$$\mathbf{AT}-\mathbf{AT_a}+\mathbf{AT_a}=\mathbf{B}+h\mathbf{T}-h\mathbf{T_a} \quad (19)$$

$$(\mathbf{A}-h)(\mathbf{T}-\mathbf{T_a})=\mathbf{B}-\mathbf{AT_a} \quad (20)$$

Eqs. (18) and (20) are the equation group for unknown variable $\mathbf{T}-\mathbf{T_a}$ and $\mathbf{T_a}$. They are again identical to Eqs. (13) and (12) because of the straightforward derivation. Iteration of $\mathbf{T}-\mathbf{T_a}$ and $\mathbf{T_a}$ between (18) and (20) can then achieve the same results as method-1.

Therefore, data exchange methods-1, -2 and -3, in fact, represent three different forms of one original equation group. They are identical mathematically, and therefore theoretically can produce the same solutions with the same set of boundary conditions (climate, geometry, etc.).

2.3.2. Numerical convergence and stability of the coupling

So far, we have verified the solution existence and uniqueness of a coupled simulation with different data exchange methods in physics and mathematics. This section will further discuss the numerical convergence and stability by using data exchange methods-1 and -2 as examples, since they are typical. The discussion continues to use the constant h assumption.

Rewrite the energy equations (15) and (17) for method-1

$$\mathbf{T}=f(\mathbf{T_a}) \quad \text{(ES)} \quad (21)$$

$$\mathbf{T_a}=g(\mathbf{T}) \quad \text{(CFD)} \quad (22)$$

The slopes for these two equations are indicated in Eqs. (6), (7), (10) and as illustrated in Fig. 4. The figure shows that a typical numerical process of method-1 will always lead to a converged point for $h>0$. However, if $h<0$, the situation becomes more complicated, as shown in Fig 5. Only if

$$\left|\frac{\partial T_a}{\partial T}\right|_{ES} > \left|\frac{\partial T_a}{\partial T}\right|_{CFD} \quad (23)$$

may the coupling have a converged solution. In fact, this is also the condition always satisfied by the case with h>0.

A similar analysis can be used for method-2. The ES and CFD equations for method-2 are

$$\mathbf{T}=f(\mathbf{Q}) \quad \text{(ES)} \quad (24)$$

$$\mathbf{Q}=g(\mathbf{T}) \quad \text{(CFD)} \quad (25)$$

Eqs. (8) and (9) indicate that the slope of Q-T curve in Eq. (24) for ES is negative while that of Eq. (25) for CFD is positive, regardless of the h value. Fig. 6 illustrates a typical

iteration of Q and T between Eqs. (24) and (25). A converged solution of the coupling can be obtained if

$$\left|\frac{\partial Q}{\partial T}\right|_{ES} > \left|\frac{\partial Q}{\partial T}\right|_{CFD} \tag{26}$$

Otherwise, the iteration may lead to divergence.

Eq. (26) can be further written as

$$\frac{\partial T_a}{\partial T}\bigg|_{ES} > 2 - \frac{\partial T_a}{\partial T}\bigg|_{CFD} > 1, \text{ when } h>0 \tag{27}$$

$$\frac{\partial T_a}{\partial T}\bigg|_{ES} < 2 - \frac{\partial T_a}{\partial T}\bigg|_{CFD} < 1, \text{ when } h<0 \tag{28}$$

If the case simulated satisfies Eqs. (27) and (28), the iteration with method-2 may converge to a solution. The iteration with method-1, however, will always unconditionally converge when h>0, and it can converge when h<0 and

$$\left|\frac{\partial T_a}{\partial T}\bigg|_{ES} > \frac{\partial T_a}{\partial T}_{CFD} > 1 \right| \tag{29}$$

In addition, data exchange method-2, in fact, performs an explicit iteration, while method-1 is an implicit iteration. Method-2 transfers $\mathbf{Q}(=h\mathbf{T}-h\mathbf{T}_a)$, instead of h and $\mathbf{T}_a$, from the last CFD (nth iteration step) to the next ES (n+1th iteration step), therefore

$$\mathbf{A}\mathbf{T}^{n+1}=\mathbf{B}+h\mathbf{T}^{n}-h\mathbf{T}^{n}_{a} \qquad \text{(ES)} \tag{30}$$

$$h\mathbf{T}^{n}-h\mathbf{T}^{n}_{a}=f(\mathbf{T}^{n}) \qquad \text{(CFD)} \tag{31}$$

It is an explicit iteration for **T** in Eq. (30). As a result, $\mathbf{T}^{n+1}$ gets updated slowly and the entire coupled simulation needs more CFD calls. Consequently, the total computing time is expected to increase.

On the contrary, method-1 performs an implicit iteration for **T** in ES by importing h and $\mathbf{T}_a$ from the last CFD.

$$\mathbf{A}\mathbf{T}^{n+1}=\mathbf{B}+h\mathbf{T}^{n+1}-h\mathbf{T}^{n}_{a} \qquad \text{(ES)} \tag{32}$$

$$h\mathbf{T}^{n}-h\mathbf{T}^{n}_{a}=f(\mathbf{T}^{n}) \qquad \text{(CFD)} \tag{33}$$

Generally, the implicit algorithm is more stable and moves on faster (hence needs less CFD calls) than the explicit algorithm, although it may need more computing effort for the iteration in ES. However, the computing time for ES is tiny compared with that for CFD. As a result, data exchange method-1 would need less computing time than method-2.

From all the analysis above, we may conclude that data exchange method-1 seems to be better than method-2. Real problems are more complicated, usually without constant slopes and highly non-linear. A theoretical analysis on those problems is impossible. Stability and convergence of real problem simulations can only be verified through numerical experiment. They will be discussed in the following section.

3. Numerical Experiments

3.1. Case Setup

To further verify the performance of coupling methods and numerical algorithms on a real building problem, it is necessary to conduct numerical experiments with some well-designed cases. The well-designed cases that can minimize the effects from other factors on convergence and stability should have the following features:

- Simple geometry
- Basic heat transfer processes
- Minimum fluctuation of outdoor environment conditions
- Controlled indoor air temperature
- Large ventilation rate attempting to avoid the spatial variation effect

Following these requirements, the study has designed an empty room as shown in Fig. 7. The cubic room (3×3×3m) is on a middle floor of a building and has only one south-facing exterior wall without windows. Table 2 lists the enclosure materials; they are the same as those in an environmental chamber. The room has no internal heat gains, and the heat load is solely due to the southern exterior wall. The outdoor air temperature was assumed to be constant at -12.8^{o}C. The room air temperature is conditioned to be constant at 23°C. A variable air volume system supplies T_{supply} = 25°C warm air from a diffuser on the north wall close to the ceiling. The exhaust outlet is on the same wall close to the floor.

3.2. Solution Performance of Iterative Coupling Methods

The three data exchange methods described in the previous section have been implemented into E+MIT-CFD, a coupled program of EnergyPlus (E+) and MIT-CFD. E+, developed by the U.S. Department of Energy, is an energy simulation program based on DOE-2 [4] and BLAST [3]. MIT-CFD is a general CFD program that solves steady and unsteady laminar and turbulent flow problems with arbitrary geometry. This section discusses the numerical experiments for the case shown in Fig. 7 with the three coupling methods.

Although the case is steady, it is necessary to perform the simulation for a few days to reach a steady state, because the assumed initial values, such as wall temperatures, are not the true values. The coupling between ES and CFD is performed only one time a day during this period. After a call to CFD, ES uses the results from CFD, such as convective heat fluxes, until it calls CFD again the next day. This one-time-step dynamic coupling is quite reasonable for the case with small variation of the influencing parameters, such as the environmental conditions and internal loads. In this case, the CFD calculation uses a coarse 12x12x14 rectangular grid and adopts both the constant viscosity and zero-equation turbulence models [31], rather than the standard k-ε turbulence module [32], to reduce the computing time of CFD. Chen and Xu's study [31] indicated that such a coarse grid and simple turbulence models can provide acceptably reasonable results for the building design purpose.

The CFD calculation uses the upwind numerical scheme to discretize the convection term and the central scheme to discretize the diffusion term. The convergence criterion for CFD requires the normalized residuals for all variables solved to be less than 1%, with a maximum iteration limit of 1000 steps per CFD run. Because the convective heat flux Q_{conv} and the interior surface temperature T_s are the linkages of ES and CFD, the difference in Q_{conv} between ES and CFD and the difference in T_s between the current and

last ES runs are used to judge the convergence of ES-CFD iterations. In fact, only one of these needs to be specified as the convergence criterion because of the inherent relationship between Q_{conv} and T_s. The present study considers the solution fully converged if the maximum difference in interior surface temperatures between two ES runs is less than 1%.

Fig. 8 shows that data exchange method-1 can lead to a converged solution in four iterations for this case. Our experience shows that convergence takes no more than 10 iterations for a more sophisticated case. Fig. 9 shows the convergence performance for three continuous days (the first two days are used to eliminate the impact of initial values on the final results). The converged solutions are reached on the second and third day in Fig. 9 (a), but not on the first day. The reason for this is that CFD needs more time steps in the startup period to obtain a converged solution.

This example shows that the iteration number is controlled by the convergence criteria. In ES-CFD coupling, both the convergence criteria for ES and CFD can be adjusted. This investigation has further tested the impact of CFD and ES convergence criteria on the computing time and accuracy of the coupled simulation with data exchange method-1. Table 3 lists different combinations of CFD and ES convergence criteria and the corresponding computing time. Test 2 and Test 5 have the best, nearly identical, performance of convergence in terms of the difference of convective heat flux on the interior surface of south wall between ES and CFD. Test 2 needs more computing time than Test 5 due to more iterations in CFD. Frequent exchange of inter-coupled information between ES and CFD is more efficient than using more iterations in a single CFD run as those cases with a smaller R_{CFD} in Table 3. However, the iteration number for each CFD run cannot be too small. For example, Test 3 and Test 6 could not yield good results. A reasonable combination of ES and CFD convergence criteria is important to quickly obtain correct results.

The numerical experiment with data exchange method-2 shows similar performance as method-1, but it needs about 30% more computing time due to the explicit iteration procedure. Data exchange method-3 can also produce a converged solution, but the solution is quite different from those by method-1 and method-2. The primary reason for this difference is because data exchange method-3 cannot properly control the indoor air temperature, which is addressed in detail as follows.

3.3. Control of Indoor Air Temperature in the Coupled Simulation

In the ES-CFD program coupling, the partial differential energy equation in CFD simulates the room air energy balance and connects with the enclosure energy balance equation in ES. Therefore, the room air energy balance equation in ES is not needed anymore. However, the ES room air energy balance equation should be used to control the indoor air temperature in the coupled simulation.

Fig. 10 illustrates the control process in the coupled simulation of the testing case by using data exchange method-1. With the constant h values provided by the constant viscosity turbulence model [20], method-1 transfers surface temperature from ES to CFD and returns indoor air temperature gradient from CFD to ES, at one specific coupling time step.

CFD first calculates the indoor air temperature distribution based on the boundary conditions (south wall interior surface temperature T=18°C from the last ES). It predicts a temperature difference 0.2°C (=24°C-23.8°C) between the calculated control point temperature $T_{control\text{-}cal}$ and the air temperature close to the surface T_a, as shown in Fig. 10. In the steady state CFD, the supply air energy requirement Q_{supply} equals the convective heat transfer Q_{conv} through the envelope, that is, $Q_{supply} = hA(T_a\text{-}T)=hA(23.8\text{-}18)$.

With this temperature gradient ($T_{control\text{-}cal}$ - T_a=0.2°C) from CFD, ES obtains the air temperature close to the surface (T_a=22.8°C) in the controlled room with the prescribed constant room air temperature (23°C). The integral energy equation in ES, therefore, produces a new $Q_{supply}=hA(T_a\text{-}T)=hA(22.8\text{-}18)$ and passes it to the next CFD run. The new Q_{supply} in CFD will drag the indoor air temperature down toward the desired air temperature. Only if $T_{control\text{-}cal}$ in CFD equals the required indoor air temperature $T_{control\text{-}set}$ in ES can the indoor air energy balance be hold in both CFD and ES.

Data exchange method-3, on the other hand, transfers Q_{conv} from ES to CFD. It results in Q_{conv}, instead of surface temperature T, being unchanged during one specific iteration step. Therefore, $T_{control\text{-}set}$ in ES will adjust T to achieve the same heat flux requirement for both ES and CFD. Consequently, both of the thermal distributions in ES and CFD can satisfy the heat balance $Q_{supply}=Q_{conv}$ and $Q_{convES}= Q_{convCFD}$ but the temperature patterns are different, as illustrated by Fig.11. The primary reason for this is that $T_{control\text{-}set}$ of ES has no relationship with the temperature field predicted by CFD. Hence, $T_{control\text{-}set}$ in ES cannot properly function as a controller for the entire coupled simulation with method-3.

To acquire correct solutions with method-3, we need to develop a new control strategy. Since in each iteration the air temperature at the outlet, T_{outlet}, needs to be transferred from CFD to ES for accurate estimation of supply air mass flow rate, one method is to create the connection between $T_{control\text{-}set}$ and the temperature field from CFD by introducing a new $T_{outlet\text{-}new}$

$$T_{outlet\text{-}new}=T_{outlet}\text{-}(T_{control\text{-}cal}\text{-}T_{control\text{-}set}) \quad (34)$$

to the next ES. However, numerical experiments show that the direct implementation of this numerical technique is quite unstable. The present investigation has proposed an improved control and iteration algorithm, consisting of three basic steps:

1. In each CFD calculation, CFD runs for up to one hundred iteration times without the requirement of convergence, because the supply air enthalpy (or, mass flow rate with a VAV system) is always updated during the coupling before reaching the final solution. The final CFD solution at each coupling step will be well converged if the boundary conditions approach the stable values.
2. The entire CFD temperature field is modified according to the difference between $T_{control\ –set}$ and $T_{control\text{-}cal}$.
3. The modified outlet temperature from CFD is used in ES to generate the new inlet supply air enthalpy for the next CFD run.

Although this new algorithm is specifically developed to solve the control problem of data exchange method-3, it is also suitable to be employed by the other methods. In fact, this algorithm should be able to accelerate the convergence for all coupling methods, because:

1. Superfluous iterations and critical criteria within each CFD run is not necessary since the boundary conditions are updated all the time.
2. The modification of the temperature field forces it to faster approach the required temperature (the control temperature in ES). The effect is similar to providing a more reasonable initial temperature field for each CFD run.
3. The modified outlet temperature, which is closer to the final result than the original CFD one without the artificial modification, helps to faster capture the correct inlet enthalpy.

The new iteration and control strategy has been implemented and used to test the three data coupling methods. Table 4 shows that all three data exchange methods can reach converged solutions, and method-1 and method-2 provide nearly identical results, as expected. Method-2 needs more computing time than method-1. Method-3 provides somewhat different solutions, because method-3 directly introduces the convective heat flux into the energy equation of CFD while method-1 and method-2 provide CFD the surface temperature, which relies on convection to affect the indoor air and thus heavily depends on the near-wall turbulence model.

The numerical experiments show that the residuals of CFD runs from the new iteration and control algorithm are smaller than those from the original one for all data exchange methods, although the iteration within each CFD calculation reduces to 100 steps. The tests with the finer convergence criteria in method-1', method-1" and method-3" verify that the solutions from method-1 and method-3 are converged and stable. The calculation with method-3' indicates that extra iterations in CFD with intermediate boundary information are not useful and may cause numerical instability.

4. Conclusions

This investigation integrated an ES program with a CFD program and studied the existence, uniqueness, convergence, and stability of the numerical solutions from the coupled program. Both the theoretical analysis and numerical experiments verify that the iteration between ES and CFD programs can lead to a correct and converged solution.

The study introduced three feasible data exchange methods to couple the two programs. Although mathematically identical, these methods have different impacts on correctness, accuracy, convergence, stability, and computing time for a coupled simulation. In general, data exchange method-1, which transfers enclosure interior surface temperatures from ES to CFD and returns convective heat transfer coefficient and indoor air temperature gradients from CFD to ES, is more stable than method-2, which transfers enclosure interior surface temperatures from ES to CFD but returns convective heat flux from CFD to ES. It is because method-1 can unconditionally satisfy the convergence condition when the heat transfer coefficient h is larger than zero. Meanwhile, the computing cost of method-2 is most expensive, since it runs explicit iteration in ES while the others are implicit. Data exchange method-3, which transfers interior convective heat flux from ES to CFD and returns convective heat transfer coefficient and indoor air temperature gradients from CFD to ES, cannot properly control indoor air temperature. This investigation has proposed an improved iterative coupling and control algorithm to solve this problem. The new algorithm also accelerates the convergence of the other coupled simulations.

References

[1] ASHRAE, ASHRAE Handbook Fundamentals, SI Edition, ASHRAE, Atlanta, 1997.

[2] S.A. Klein, J.A. Duffie, W.A. Beckman, TRNSYS - A transient simulation program, ASHRAE Transaction 82 (1976) 623.

[3] D.C. Hittle, Building loads analysis and system thermodynamics (BLAST) users manual (Version 2.0), Technical Report E-153, Vol. 1 and 2, U.S. Army Construction Engineering Research Laboratory (USA-CERL), Champaign, IL, 1979.

[4] B.E. Birdsall, et al., The DOE-2 computer program for thermal simulation of buildings, Energy Sources: Conservation and Renewables, American Institute of Physics, Ed. David Hafmeister, 1985.

[5] J.A. Clarke, Energy simulation in building design, Adam Hilger, Bristol, 1985.

[6] D.B. Crawley, L.K. Lawrie, C.O. Pedersen, F.C. Winkelmann, EnergyPlus: energy simulation program, ASHRAE Journal 42 (4) (2000) 49-56.

[7] J. Lebrun, Exigences physiologiques et modalités physiques de la climatisation par source statique concentrée, PhD Thesis, University of Liège, 1970.

[8] E. Mundt, The performance of displacement ventilation systems - experimental and theoretical studies, PhD Thesis, Royal Institute of Technology, Stockholm, 1996.

[9] X. Yuan, Q. Chen, L.R. Glicksman, Models for prediction of temperature difference and ventilation effectiveness with displacement ventilation, ASHRAE Transactions 105 (1) (1999) 353-367.

[10] S.J. Rees, P. Haves, A nodal model for displacement ventilation and chilled ceiling systems in office spaces, Building and Environment 36 (2001) 753-762.

[11] P. Dalicieux, H. Bouia, Présentation d'une modélisation simplifiée desmouvements d'air à l'intérieur d'une pièce d'habitation, Electricite de France Report (EDF) rep. HE 12 W 3269, 1991.

[12] C. Inard, H. Bouia, P. Dalicieux, Prediction of air temperature distribution in buildings with a zonal model, Energy and Buildings 24 (1996) 125-132.

[13] E. Wurtz, J-M. Nataf, F. Winkelmann, Two- and three-dimensional natural and mixed convection simulation using modular zonal models in buildings, International Journal of Heat and Mass Transfer 42 (1999) 923-940.

[14] F. Haghighat, Y. Lin, A.C. Megri, 2001. Development and validation of a zonal model – POMA, Building and Environment 36 (2001) 1039-1047.

[15] B. Griffith, Incorporating nodal and zonal room air models into building energy calculation procedures, Master Thesis, Massachusetts Institute of Technology, 2002.

[16] F. Ladeinde, M. Nearon, CFD applications in the HVAC&R industry, ASHRAE Journal 39(1) (1997) 44.

[17] S.J. Emmerich, Use of computational fluid dynamics to analyze indoor air quality issues, National Institute of Standards and Technology report NISTIR 5997, USA, 1997.

[18] P.V. Nielsen, The selection of turbulence models for prediction of room airflow, ASHRAE Transactions 104(B) (1998) 1119-1127.

[19] Q. Chen, X. Peng, A.H.C. van Paassen, Prediction of room thermal response by CFD technique with conjugate heat transfer and radiation models, ASHRAE Transactions 3884 (1995) 50-60.
[20] Z. Zhai, Q. Chen, P. Haves, J.H. Klems, On approaches to couple energy simulation and computational fluid dynamics programs", Building and Environment (2002) (in press).
[21] Q. Chen, J. van der Kooi, ACCURACY - a computer program for combined problems of energy analysis, indoor airflow and air quality, ASHRAE Transactions 94(2) (1988) 196-214.
[22] J.A. Clarke, W.M. Dempster, C.O.R. Negrao, The implementation of a computational fluid dynamics algorithm within the ESP-r system, Proceedings of Building Simulation '95, Madison, USA, International Building Performance Simulation Association, 1995, pp. 166-75.
[23] C.O.R. Negrao, Conflation of computational fluid dynamics and building thermal simulation, PhD Thesis, University of Strathclyde, Glasgow, UK, 1995.
[24] P.V. Nielsen, T. Tryggvason, 1998. "Computational fluid dynamics and building energy performance simulation," Proceedings of Roomvent '98, Vol. 1, Stockholm Sweden, 1998, pp. 101-107.
[25] J. Srebric, Q. Chen, L.G. Glicksman, A coupled airflow-and-energy simulation program for indoor thermal environmental studies, ASHRAE Transactions 106(1) (2000) 465-476.
[26] I. Beausoleil-Morrison, The adaptive coupling of heat and air flow modeling within dynamic whole-building simulation, PhD Thesis, University of Strathclyde, Glasgow, UK, 2000.
[27] R.M. Clovis, Issues on the integration of CFD to building simulation tools," Seventh International IBPSA Conference (BS2001), Vol. 1, Rio de Janeiro, Brazil, August, 2001, pp. 29-40.
[28] J.A. Clarke, J.L.M. Hensen, C.O.R. Negrao, Predicting indoor air flow by combining network approach, CFD and thermal simulation, Proceedings of 16th AIVC Conference, 1995, pp. 145-53.
[29] J.H. Klems, Shape of T_S vs Q_C curves, private communications, Lawrence Berkeley National Laboratory, 1999.
[30] I.S. Duff, A.M. Erisman, J.K. Reid, Direct methods for sparse matrices, Oxford Science Publication, 1986.
[31] Q. Chen, W. Xu, A zero-equation turbulence model for indoor airflow simulation, Energy and Buildings 28 (1998) 137-144.
[32] B.E. Launder, D.B. Spalding, The numerical computation of turbulent flows, Computer Methods in Applied Mechanics and Energy 3 (1974) 269-289.

Table 1 Changes of $Q_{conduction}$, $Q_{radiation}$, and $Q_{convection}$ with interior surface temperature T

	T	Q_{cond}	Q_{rad}	Q_{conv} ($=Q_{cond}- Q_{rad}$)		T	$-Q_{cond}$	$-Q_{rad}$	$-Q_{conv}$ ($=-Q_{cond}+ Q_{rad}$)
Summer	↑	↓	↑	↓	Winter	↑	↑	↓	↑

Table 2 Room enclosure materials

Enclosure	Thickness (m)	Density (kg/m^3)	Specific heat (J/kgK)	Thermal conductivity (W/mK)
Ceiling/Floor	0.175	2300	840	1.9
Walls	0.140	700	840	0.23

Table 3 Comparison for different convergence criteria with data exchange method-1

	Convergence Criteria	$T_{RoomCFD}$ (C)	$Q_{surfaceES}$ (W/m^2)	$\Delta Q_{surface}$ (W/m^2)	Time (s)
Test 1	R_{CFD}<0.01 , R_{ES}<0.01	22.80	23.4	0.8	68
Test 2	R_{CFD}<0.001, R_{ES}<0.01	22.95	24.6	0.2	403
Test 3	R_{CFD}<0.1 , R_{ES}<0.01	22.60	15.9	1.1	98
Test 4	R_{CFD}<0.01 , R_{ES}<0.001	22.88	25.0	0.5	81
Test 5	R_{CFD}<0.01 , R_{ES}<0.0001	22.96	24.6	0.2	138
Test 6	R_{CFD}<0.1 , R_{ES}<0.0001	22.88	13.7	0.3	48
Test 7	R_{CFD}<0.001, R_{ES}<0.1	22.87	25.1	0.1	274

Note: $T_{roomCFD}$ – room air temperature obtained from CFD; $Q_{surfaceES}$ – convective heat flux at south wall obtained from ES; $\Delta Q_{surface}$= $Q_{surfaceES}$- $Q_{surfaceCFD}$; $Q_{surfaceCFD}$ – convective heat flux at south wall obtained from CFD; Time: computing time.

Table 4 Results comparison for different coupling methods with new iteration and control algorithm (zero-equation turbulence model, upwind scheme, IterCFD=100 or R_{CFD}<0.1%, R_{ES}<1%)

	Q_{total} (W)	Q_{surfES} (W/m^2)	$Q_{surfCFD}$ (W/m^2)	ΔQ_{surf} (W/m^2)	$T_{southES}$ (C)	$T_{southCFD}$ (C)	h_{south} (W/m^2K)	R_{CFD} (<)	Time (s)
Method-1	383	23.94	23.99	0.05	18.04	18.04	4.84	0.23%	85
Method-2	384	24.08	24.03	0.05	18.04	18.04	4.85	0.11%	109
Method-3	308	19.33	19.33	0.00	17.54	17.55	3.52	0.55%	108
Method-3’	283	17.94	17.94	0.00	17.66	17.62	3.31	0.50%	459
Method-3”	308	19.39	19.39	0.00	17.56	17.56	3.54	0.19%	199
Method-1’	409	25.18	25.14	0.04	17.97	17.97	5.04	0.10%	144
Method-1”	385	24.09	24.06	0.03	18.05	18.05	4.87	0.10%	105

Note:
’ means the change of IterCFD=100 or R_{CFD}<0.1% to IterCFD=500 or R_{CFD}<0.1%;

" means the change of R_{ES}<1% to R_{ES}<0.1%.
Q_{total} – total energy requirement for space; Q_{surfES} – convective heat flux at south wall from ES; $Q_{surfCFD}$ – integral convective heat flux at south wall from CFD; ΔQ_{surf}= Q_{surfES}- $Q_{surfCFD}$; $T_{roomCFD}$ – control room air temperature in CFD; $T_{southES}$ – south wall surface temperature from ES; $T_{southCFD}$ – south wall surface temperature from CFD; h_{south} – convective heat transfer coefficient at south wall; R_{CFD} – final residuals in CFD; Time – computing time.

Fig. 1 T_a-T curve of ES and CFD

Fig. 2 q_c-T curve of ES and CFD

Fig. 3 Multiple Intersections between T_a-T curves of ES and CFD (h>0)

Fig. 4 Converged iteration process of coupling ES with CFD in T_a-T plot (h>0)
(ES provides T to CFD as boundary conditions, and then CFD returns a new T_a to ES. The process repeats and a converged point can be reached finally.)

Fig. 5 Iteration process of coupling ES and CFD in T_a-T plot (h<0)
(ES provides T to CFD as boundary conditions, and then CFD returns a new T_a to ES.)

Fig. 6 Iteration process of ES and CFD in q_c-T plot
(a) with $\left|\partial q_c/\partial T\right|_{ES} > \left|\partial q_c/\partial T\right|_{CFD}$ and (b) with $\left|\partial q_c/\partial T\right|_{ES} < \left|\partial q_c/\partial T\right|_{CFD}$
(CFD provides q_c to ES, and ES returns a new T for CFD as boundary conditions.)

Fig. 7. The air velocity (a) and temperature (b) distributions at the middle section of the room (V_{supply}=0.78m/s; T_{supply}=25°C)

Fig. 8. A typical convergence process of E+CFD-MIT with coupling method-1 for a particular time step.

Fig. 9 Convergence of one-time-step dynamic coupling for three continuous days with data exchange method-1 and 0-equation turbulence model
(Top (a): CFD residuals<0.01; Bottom (b): CFD residuals<0.001)

Fig. 10 Control process of indoor air temperature in the coupled simulation with data exchange method-1

Fig. 11 Control process of indoor air temperature in the coupled simulation with data exchange method-3

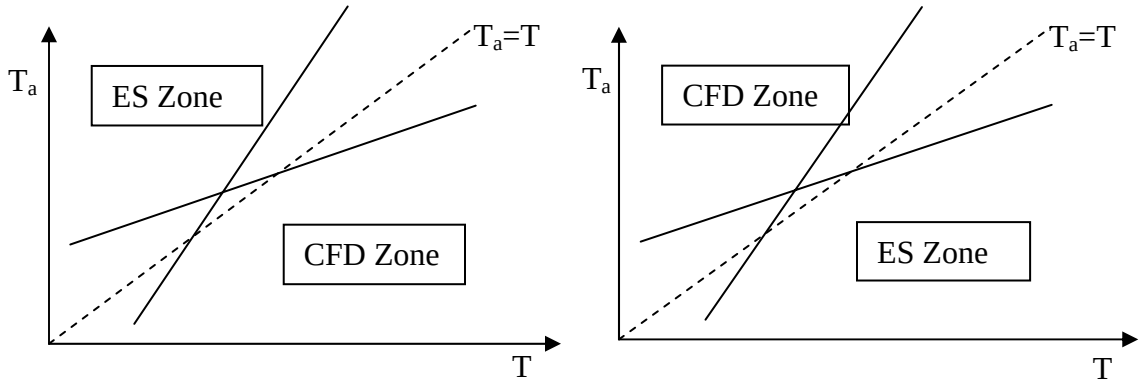

(a) h>0 (b) h<0

Fig. 1 T_a-T curve of ES and CFD

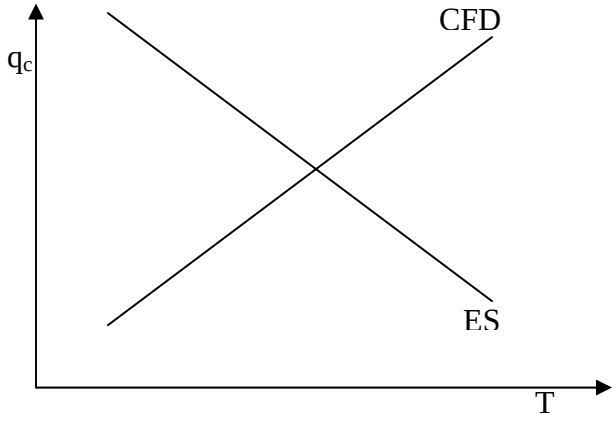

Fig. 2 q_c-T curve of ES and CFD

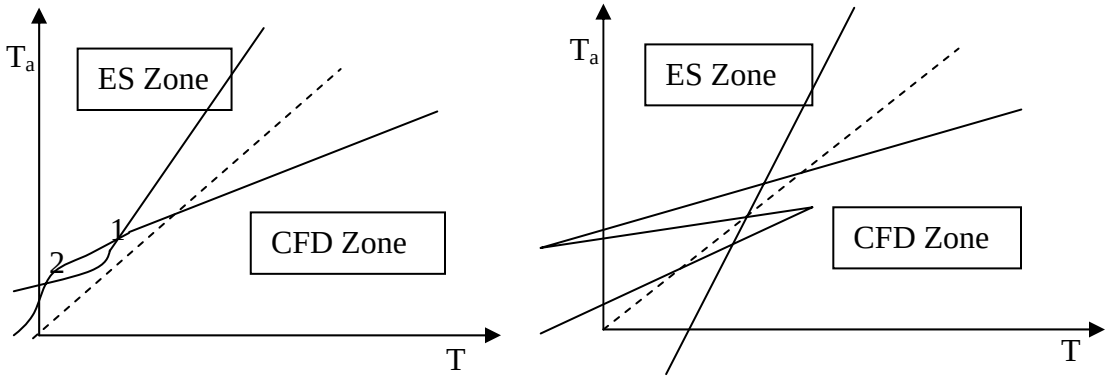

Fig. 3 Multiple Intersections between T_a-T curves of ES and CFD (h>0)

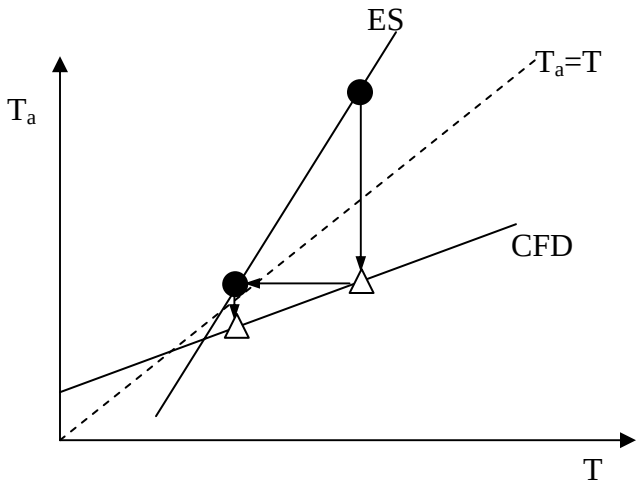

Fig. 4 Converged iteration process of coupling ES with CFD in T_a-T plot (h>0)
(ES provides T to CFD as boundary conditions, and then CFD returns a new T_a to ES.
The process repeats and a converged point can be reached finally.)

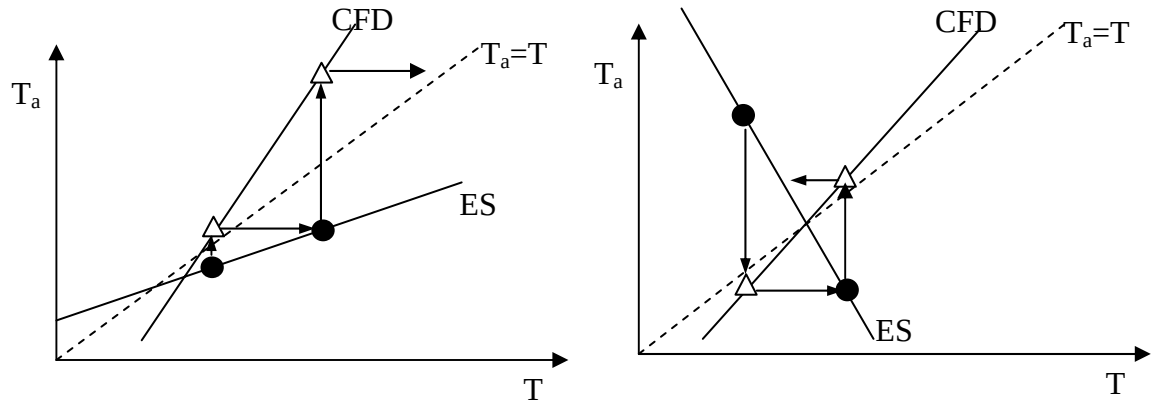

(a) Diverged (b) Converged

Fig. 5 Iteration process of coupling ES and CFD in T_a-T plot (h<0)
(ES provides T to CFD as boundary conditions, and then CFD returns a new T_a to ES.)

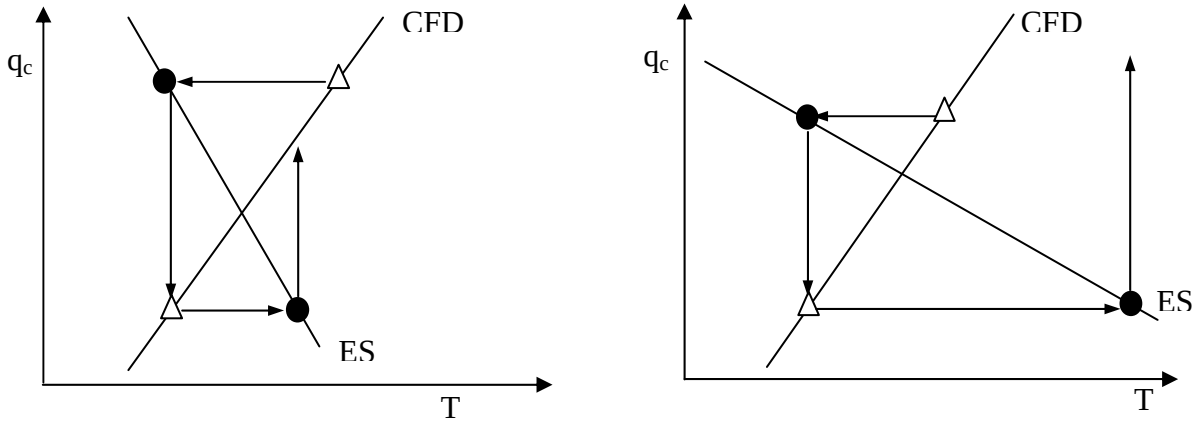

(a) Converged (b) Diverged

Fig. 6 Iteration process of ES and CFD in q_c-T plot
(a) with $\left|\partial q_c/\partial T\right|_{ES} > \left|\partial q_c/\partial T\right|_{CFD}$ and (b) with $\left|\partial q_c/\partial T\right|_{ES} < \left|\partial q_c/\partial T\right|_{CFD}$
(CFD provides q_c to ES, and ES returns a new T for CFD as boundary conditions.)

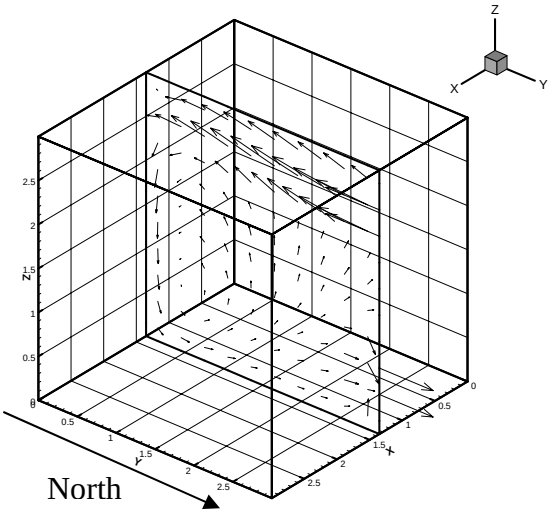

(a)

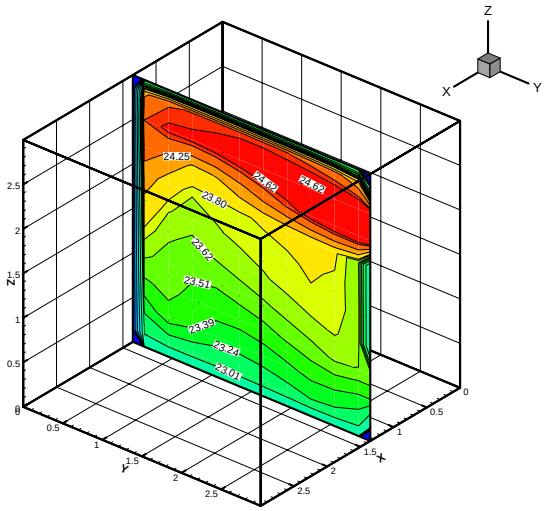

(b)

Fig. 7. The air velocity (a) and temperature (b) distributions at the middle section of the room (V_{supply}=0.78m/s; T_{supply}=25°C)

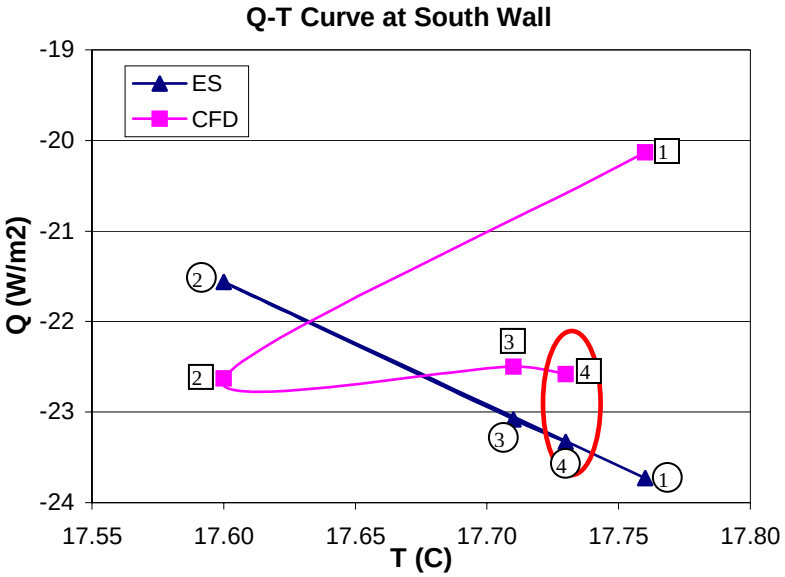

Fig. 8. A typical convergence process of E+CFD-MIT with coupling method-1 for a particular time step.

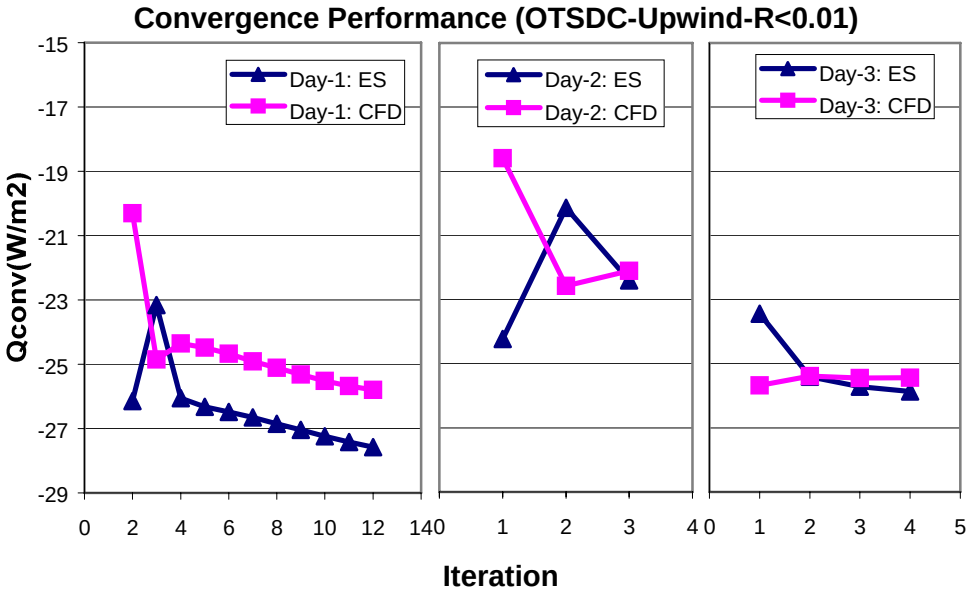

[Computing time = 64 seconds]

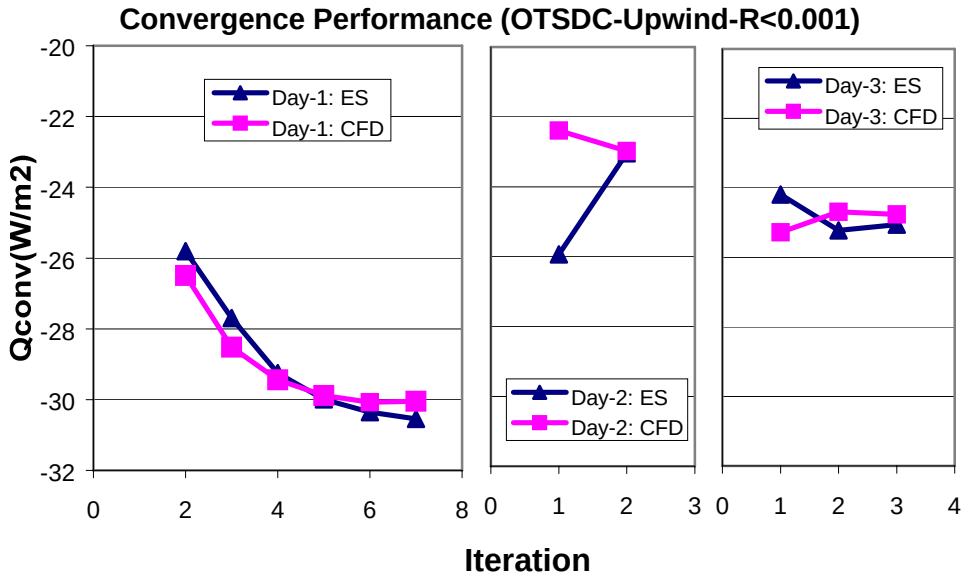

[Computing time = 351 seconds]

Fig. 9 Convergence of one-time-step dynamic coupling for three continuous days with data exchange method-1 and 0-equation turbulence model
(Top (a): CFD residuals<0.01; Bottom (b): CFD residuals<0.001)

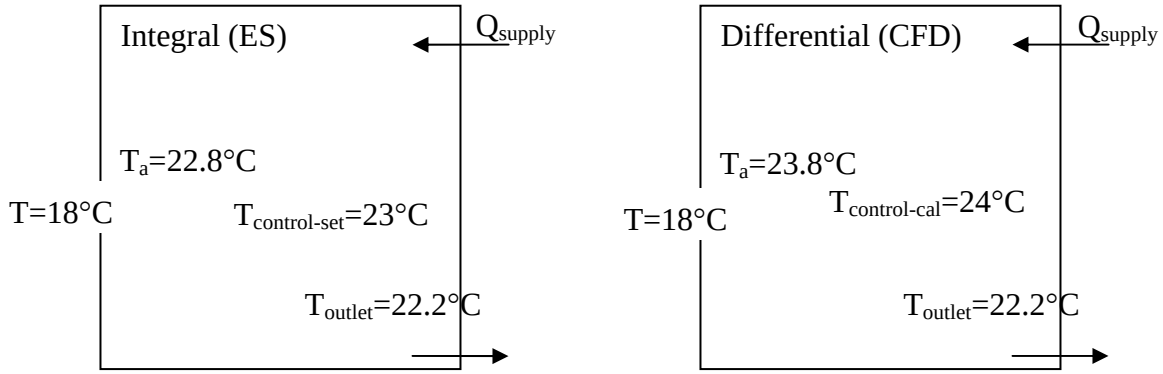

Fig. 10 Control process of indoor air temperature in the coupled simulation with data exchange method-1

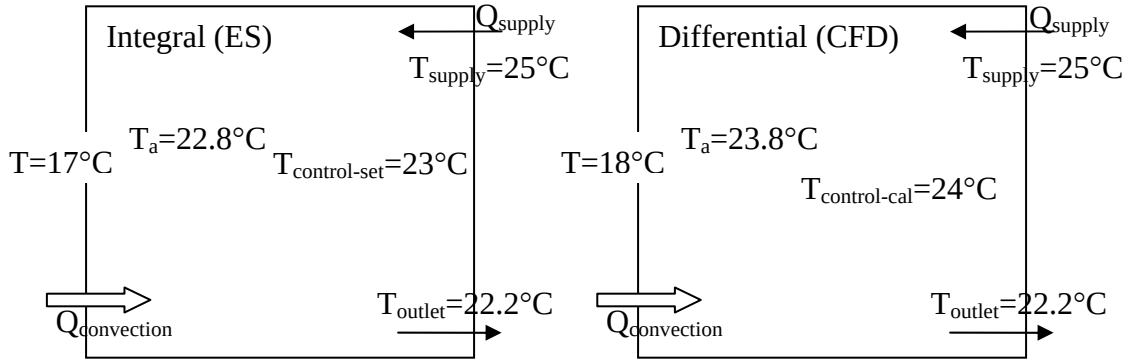

Fig. 11 Control process of indoor air temperature in the coupled simulation with data exchange method-3